Microstructure, Mechanical and Corrosion Behaviour of AA7075 Aluminium Alloy Friction Stir Welds

P. Vijaya Kumar [a], G. Madhusudhan Reddy [b], K. Srinivasa Rao [c]

[a] Department of Mechanical Engineering, Raghu Institute of Technology, Visakhapatnam, India

[b] Defence Metallurgical Research Laboratory, Hyderabad, India

[c] Department of Metallurgical Engineering, Andhra University, Visakhapatnam, India

Corresponding Author: vijay.mech@raghuinstech.com

DOI : 10.22486/iwj/2018/v51/i2/170312

ABSTRACT

Friction stir welding (FSW) is emerging as an alternative technique for joining high strength aluminium alloys as it eliminates the problems during fusion welding. In this work, the effect of post weld treatments (PWHT), viz., peak aging (T6) and retrogression and reaging (RRA) on the microstructure, mechanical properties, pitting corrosion and stress corrosion cracking (SCC) resistance of AA7075 aluminium alloy friction stir welds has been studied. An attempt also has been made to change the chemical composition of the weld nugget by adding boron carbide (B_4C) nano powder with the aid of the FSW. Hardness and tensile properties were found to be better in PWHT – T6. Pitting corrosion and SCC resistances were improved in PWHT-RRA condition with negligible loss of strength when compared to PWHT-T6. RRA promotes coarse precipitation of the equilibrium phase η in the grains and sub grain boundaries, while maintaining a fine distribution of η' in the grain interiors. The increased strength and hardness in the peak aged (T6) condition was attributed to the presence of semi-coherent intermediate η' ($MgZn_2$). With the addition of B_4C nano powder to the weld nugget, hardness, tensile properties, pitting corrosion resistance and SCC resistance were further improved significantly when compared to the unreinforced weld nugget. PWHT- RRA treatment on the welds with B_4C nano powder addition resulted in improved hardness of weld nugget which is attributed to the uniform distribution of strengthening precipitates in the matrix and powder strengthening. Pitting corrosion resistance, Tensile strength and SCC resistance was improved significantly in B_4C added welds after RRA treatment when compared to the same welds without B_4C addition.

Keywords: Friction stir welding; FSW; AA7075 aluminium alloy; Pitting corrosion; Stress corrosion cracking; Retrogression-reaging; RRA; boron carbide (B_4C).

1.0 INTRODUCTION

High strength aluminium alloys are extensively used in defense, military, aerospace, marine and other harsh environments. AA7075 alloy in welded form show poor mechanical properties due to the defects like brittle dendritic structure, porosity, distortion and residual stresses, alloy segregation, hot cracking and hydrogen entrapment during fusion welding. These problems are eliminated by Friction stir welding (FSW) which is an autogenous solid state welding technique. FSW is an energy efficient, environment friendly process and it has many advantages like grain refinement, low heat input, low residual stresses etc. But the corrosion resistance of AA7075 aluminium alloy friction stir welds is less. Corrosion resistance of these welds is poor due to microstructural variation and softening at heat effected zone. In addition, abnormal grain growth and thermal cycles, wide precipitate free zones (PFZs) and coarse precipitates are the causes for poor corrosion resistance of weld nugget (WN). Corrosion resistance of these welds can be improved by post weld heat treatments (PWHT), welding at optimized welding conditions, underwater FSW and in-process cooling, etc. The dissolution of Cu-Zn rich precipitates the grain boundaries in the weld nugget zone also contributes to corrosion in WN. Several post weld heat treatments such as overaging (T73),

Peak aging (T6), Retrogression, and Retrogression-Reaging (RRA) are currently in practice. T6 treatment gives improved mechanical properties of welds but the corrosion resistance is poor in the welds after treating to T6. RRA improves the corrosion resistance of the welds without impairing the mechanical properties. As these welds have to serve in defense and variable loading environments, there a need of further improvement of weld strength and corrosion resistance. Changing the chemical composition of the weld nugget by the addition of nano ceramic powders like boron carbide (B_4C) can further improve the strength and corrosion resistance of WN.

Present study is significant as the studies on microstructure, mechanical properties and stress corrosion cracking (SCC) of AA7075 alloy friction stir welds with the addition of B_4C nano powders have not been reported so far. B_4C was chosen for reinforcement due to its density (2.52 g/cm^3) and elastic modulus of (427 GPa). In view of the above facts, the present work has been aimed to improve the microstructure, SCC resistance, hardness, and tensile properties of the friction stir welds of AA7075 alloy by using post weld heat treatments viz. T6, RRA and addition of boron carbide (B_4C) nano powder.

2.0 EXPERIMENTAL DETAILS

The AA7075 aluminium alloy plate was friction stir welded using optimum welding process parameters. The process parameters used for the welding are given in **Table 1**.

The dimensions of the rolled AA7075 plate are 240 mm X 150 mm X 8 mm. The chemical composition of base metal is given in **Table 2**.

The top surface of the plate was drilled with 1 mm diameter drill at a distance of 2 mm in a zigzag form, as shown in **Fig. 1**. The holes are drilled along the length of the tool travel on the plates. The depth of the holes was 4 mm. The 60 nm-sized B_4C powder was filled in the drilled holes made on the plates. Initially the powder-filled holes of the plates were closed with the help of friction stir processing (FSP) tool. After processing with FSP tool, the processed region was then friction stirred with FSW tool. The FSP and FSW tools used for making the joint with the nano powder are shown in **Fig. 1.**

The schematic representation of plates with holes for FSW is shown in **Fig.1**. The samples for metallography, hardness measurement, tensile testing, pitting corrosion tests and stress corrosion cracking (SCC) tests were extracted from the welded plates with and without the addition of B_4C powder. All the samples are heat treated to peak aging (T6) and RRA conditions given in **Table 3**.

Peak aged treatment (T6) is a solution treatment applied to aluminium alloys as per the standards ASTM B807/B807M. The RRA process was first developed by Cina and Gan [13, 14] in the mid-1970s and was further developed by Oliveira et al. [15] at the National Research Council of Canada (NRC). T6 and RRA

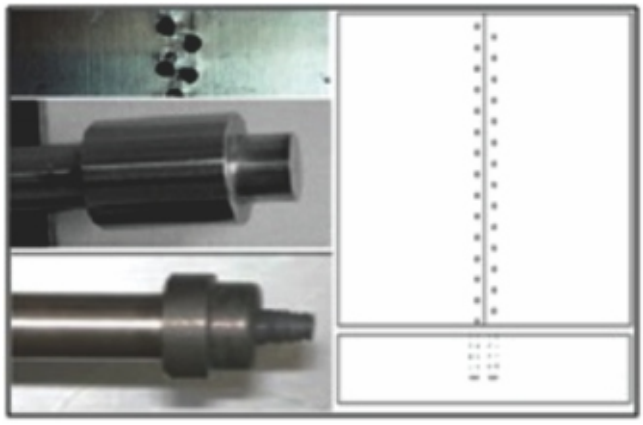

Fig.1 : Tools and preparation of plates used for addition of B_4C nano powders.

Table 1 : Process parameters of Friction Stir Welding

Process parameters	Spindle Speed (rpm)	Tool Down Feed (mm/min.)	Depth (mm)	Initial Heat Time (Sec.)	Tool Axial Feed (mm/min.)	Tool Longitudinal Travel (mm)
Values	750	40	7.25	3	25	240

Table 2 : Chemical composition (wt. %) of the 7075 aluminium alloy

Zn	Mg	Cu	Fe	Si	Ti	Mn	Cr	Al	Other
5.6	2.5	1.5	0.5	0.4	0.2	0.3	0.25	87.1-91.4	0.15

Table 3 : Post weld heat treatment procedures used on friction stir welds

Temper Condition		Ageing Temperature
T6	Near peak aged	Solution heat treatment at 515^{0}C for 1.5hrs with cold water quench and heating at 120^{0}C for 24hr.
Retrogression and Re-ageing (RRA)	Peak aged	Heat treatment at 220^{0}C for 5mins, then water quenched and again aged at T6 condition.

treatments are applied to the AA7075 aluminium base alloy and the friction stir welds. Optical microscopy (OM) has been performed on the heat treated samples as per ASTM-E3 (95).

The microstructures were recorded with image analyzer. Scanning electron microscopy (SEM) analysis was carried out on the samples to study the grain structure and precipitates as per ASTM-E340. The hardness of the samples is measured by using Vickers hardness tester with 0.5 kg f of load and 15 s of dwelling time (ASTM-E384). Tensile tests were conducted as per ASTM-E8/E8M on the prepared samples after the heat treatment. A software-based potentio-dynamic polarization test was performed on the post weld treated samples of the friction stir welds as well as the heat treated base metal in order to study the effect of post weld heat treatments on pitting corrosion behavior of the alloy. A saturated calomel electrode (SCE) and a carbon electrode were used as reference and auxiliary electrodes, respectively. All experiments were conducted in aerated 3.5% NaCl solutions with PH adjusted to 10 by adding potassium hydroxide. The potential scan was carried out at 0.166 Mv/s with the initial potential of -0.25 V (OC) SCE to the final pitting potential. The exposure area for these experiments was 1 cm^2. Pitting corrosion testing has been done as per ASTM-G34. The potential at which current increased drastically was considered to be the critical pitting potential, E_{pit}. The samples exhibiting relatively more passive potentials (or less negative potentials) were considered to have better pitting corrosion resistance. Optical microscopy on dynamically polarized samples was carried out to understand the mechanism of pitting. Stress corrosion cracking tests were conducted on constant load type SCC testing setup as per ASTM E-8/E8M-09 standards. SCC samples of base metal, as-welded and post weld heat treated at T6, and RRA were loaded as shown in the **Fig. 2**.

The load applied on the test specimens were based on tensile test results and 50% of the yield strength was applied as load on SCC specimens. SCC specimens were immersed in a 3.5 wt.% NaCI solution (pH 6.5-7.0) and the solution was periodically circulated to maintain a constant pH. The load

Fig. 2 : SCC Test setup

applied and the time to failure was recorded for each specimen. 30 mm-sized B_4C powder was ball-milled in a high energy planetary ball mill in wet mode using toluene as a liquid medium for 15 h. After the ball milling, the particle size was measured with XRD and was found to be 60 nm.

3.0 RESULTS AND DISCUSSIONS

3.1 Microstructure

Fig. 3 and **Fig. 4** show the WN microstructures of friction stir welds without B_4C powder addition and with B_4C addition.

SEM images of the same are represented in the **Fig. 5** and **Fig. 6**. Fine and equi-axed recrystallized grain structure in the nugget was developed due to tool stirring action and temperature. From the **Fig.3** and **Fig.5**, the presence of some intermetallics can be observed. These intermetallics have been

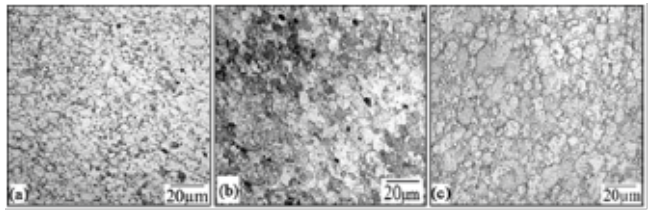

Fig. 3 : Optical micrographs of nugget zone without B_4C addition: (a) As-welded (b) PWHT-T6 (c) PWHT-RRA.

previously identified as mainly Al_7Cu_2Fe, $(Al, Cu)_6(Fe, Cu)$, and Mg_2Si. In PWHT-T6 sample **(Fig. 5 b)** of WN the microstructure contains the constituents such as GP zones, semi-coherent η ($MgZn_2$), and incoherent η ($MgZn_2$) precipitates. High strength of T6 microstructure is mainly due to GP zones and η' precipitates, but the contribution of η' precipitates to the strength was reported to be higher. In RRA sample **(Fig. 5 c)** segregations are formed in the order, GP zones →η' →η.

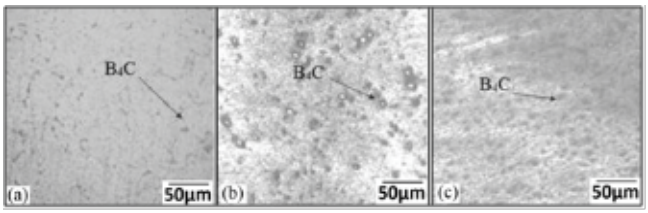

Fig. 4 : Optical micrographs of nugget zone with the B_4C addition: (a) As-welded (b) PWHT-T6 (c) PWHT-RRA.

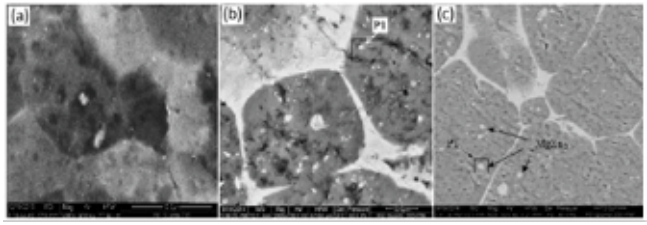

Fig. 5 : SEM images of weld nugget without B_4C addition: (a) As-welded (b) PWHT-T6 (c) PWHT-RRA.

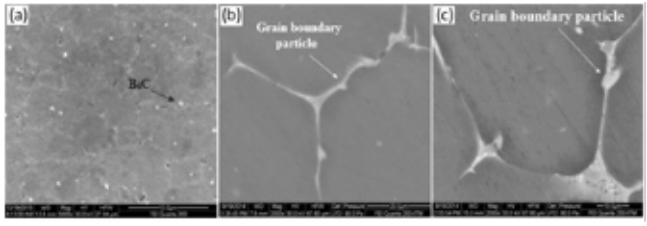

Fig. 6 : SEM images of weld nugget with B_4C addition: (a) As-welded (b) PWHT-T6 (c) PWHT-RRA.

The microstructure of the nugget zone with B_4C nano powder reinforcement (**Fig. 4** and **Fig. 6**) shows the dynamic recrystallization due to severe plastic deformation. The finely dispersed B_4C nano particles are accumulated at the grain boundaries of the welds. These reinforcement particles at the grain boundaries along with the strengthening precipitates ($MgZn_2$, Mg_3Zn) are the main contributors to the improvement of hardness and corrosion resistance. The movement of dislocations in the matrix is arrested more effectively by the nano B_4C particles. The size of the B_4C particles was further reduced due to the tool force and the stirring action. These finer particles also restrict the grain growth in the WN. There was no significant grain growth in the nugget zone as the reinforcement particles acted as barriers to the grain boundary migration **(Fig. 6)**. Uniform and continuous fine grain structure and the presence of particle rich and strengthening precipitates at the grain boundaries are the causes of increased hardness **(Fig. 6b)** in PWHT-T6 sample with B_4C addition. In B_4C added, PWHT-RRA sample **(Fig. 6c)**, the grain boundaries were discontinuous and the reinforcement particles were dispersed around the grain boundaries. Grain coarsening was also observed. The particle rich and particle free regions can be seen in the RRA sample due to the development of non uniform grain structure. The particle free region undergoes the grain growth and the particle rich region resists the grain growth.

3.2 Hardness

From **Table 4** and **Fig. 7**, the hardness of nugget zone is relatively low and may be attributed to the softening of the nugget zone and the dissolution and distribution of strengthening precipitates.

It is evident that, after PWHT, the hardness was high in peak aged condition (T6) in the nugget zone of the welds. The

Table 4 : Vickers Hardness values

Sample	Vickers Hardness values (VHN)	
	Welds without B_4C	Welds with B_4C [60 nm]
Base metal	150	
As welded	140	168
T6	170	196
RRA	145	180

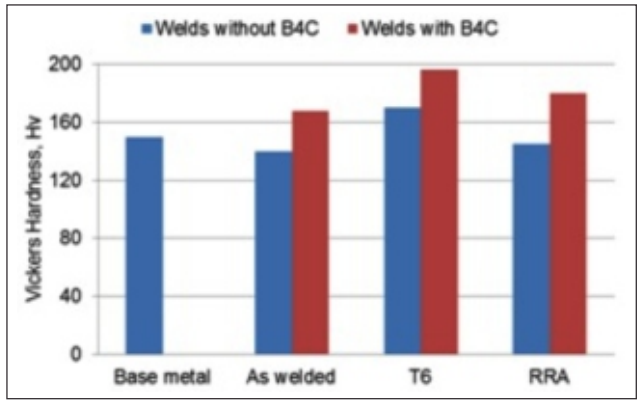

Fig. 7 : Variation of hardness

hardness was improved significantly with the addition of nano B_4C nano powder in the nugget zone (WN). These B_4C particles acts as reinforcement particles in WN and are agglomerated at the grain boundaries, leading to the improvement of the hardness. With RRA treatment on FSW AA7075 alloy without B_4C addition, there was a slight reduction in the hardness values.

Reduction in hardness may be attributed to the dissolution of GP zones during retrogression and growth and segregation of η' phase during subsequent reaging. The hardness difference between the T6 and RRA conditions in WN with the addition of B_4C nano powder was very less. When hard nano powders are added to the base aluminum alloy with the aid of FSW, the fine particles are expected to be agglomerated and uniformly distributed in the nugget region of the joint. In the present investigation, the reinforcement of B_4C nano particles in the weld nugget improved the hardness significantly, and the hardness in RRA condition is very close to that in T6 condition.

3.3 Pitting corrosion

Pitting potential values of weld nugget zone with and without B_4C nano powder are given in **Table 5**. Resistance to pitting corrosion was improved in the weld nugget formed by reinforcing B_4C particles.

Hard B_4C particles act as insulators and prevent the galvanic coupling between the matrix and the precipitates, thereby improving the resistance to pitting corrosion. Pitting corrosion resistance was found to be improved significantly by the addition of B_4C nano particles. The density of finer particles also increases the chances of segregation at the grain boundaries, thereby improving the resistance to pitting corrosion. There was a significant improvement of pitting corrosion resistance in RRA condition due to the combined effect of reinforcements and microstructural changes of the nugget due to RRA treatment. Redistribution of grain boundary precipitates, elimination of PFZs and more number of coherent precipitates in the matrix are the microstructural features that help in improving the pitting corrosion resistance.

Table 5 : Pitting potential values (mV) of base metal and nugget zone

Sample	Pitting Potential Values (mV)	
	Welds without B_4C	Welds with B_4C [60 nm]
Base metal	-740	
As welded	-855	-818
T6	-851	-815
RRA	-854	-505

3.4 Tensile and SCC tests

Tensile properties of the FSW joints are dependent on the microstructure which in turn depends on the welding conditions, base metal initial temper conditions and post weld treatments. Tensile properties of AA7075 base metal and friction stir welds in as-welded and post weld heat treated condition are given in **Table 6**.

Table 6 : Tensile properties of AA7075 base metal and friction stir welds in different conditions.

Sample Condition	Yield Strength (Y.S.) (MPa)	Ultimate Tensile Strength (UTS), (MPa)	% Elongation
Without B_4C powder addition			
Base Metal	421	482	8.4
As-welded	480	560	8
PWHT-T6	365	415	9.4
PWHT-RRA	455	540	11.2
With B_4C powder addition			
As-welded	286	374	5.5
PWHT-T6	471	579	5.1
PWHT-RRA	465	572	9.7

Table 6 Tensile properties of AA7075 base metal and friction stir welds in different conditions.

The stress-strain curves of base alloy and weld samples in different post weld heat treated conditions are shown in **Fig. 8** and **Fig. 9**. Tensile properties of the joints obtained by FSW without and with B_4C nano powder addition to weld nugget in as-welded and PWHT conditions are summarized in **Table 6**. It is evident from the above results that the post weld heat treatments significantly influence the tensile properties of FSW joints. RRA treatment improved the tensile properties of the FSW joint compared to the as-welded condition.

As-welded sample with B_4C addition had shown higher strength than the same weld without B_4C addition. Increased strength of the joint is due to the reinforcement of B_4C particles in the weld nugget. Post weld heat treatments to peak aged (T6) and RRA increased the tensile strength of the friction stir welded joints. Further, with addition of B_4C powder to the weld nugget by FSW further increased the weld strength in post weld heat treated samples due to the combined effect of post weld heat treatment and B_4C particle addition.

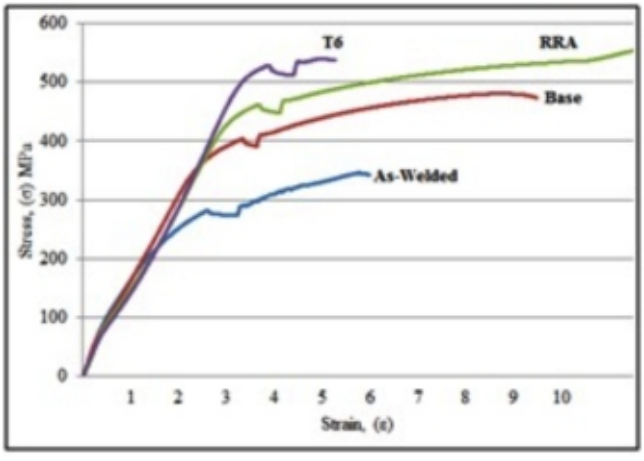

Fig.8 : Stress-strain curves of AA7075 aluminium alloy friction stir welds in different conditions

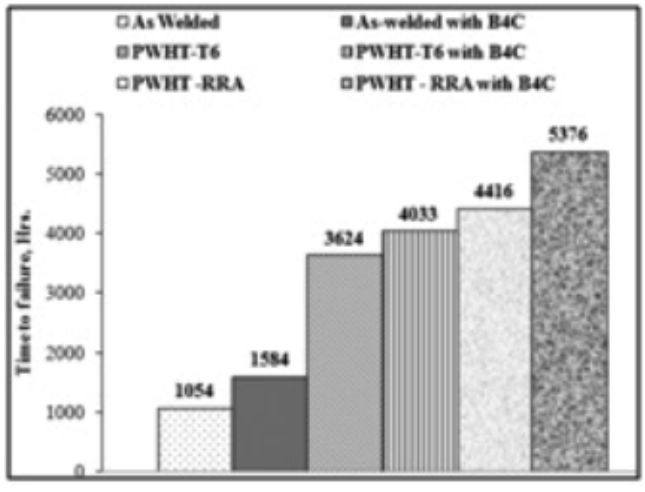

Fig. 10 : Failure times for SCC samples of AA7075alloy, welds with and without B_4C addition

However the strength of the joint in PWHT-T6 condition is slightly more than the strength of the joint in PWHT-RRA sample.

SCC tests were conducted on the friction stir welds without and with B_4C nano powder addition. SCC samples in as-welded, PWHT-T6 and PWHT-RRA conditions are examined. Loading of the SCC samples was done with 50% of the yield strength of the samples obtained in the tensile tests. Failure times for SCC samples of welds are shown in the **Fig. 10**. Failure time for PWHT – T6 with B_4C addition shown longer time than the same sample without B_4C addition. B_4C added PWHT-RRA sample

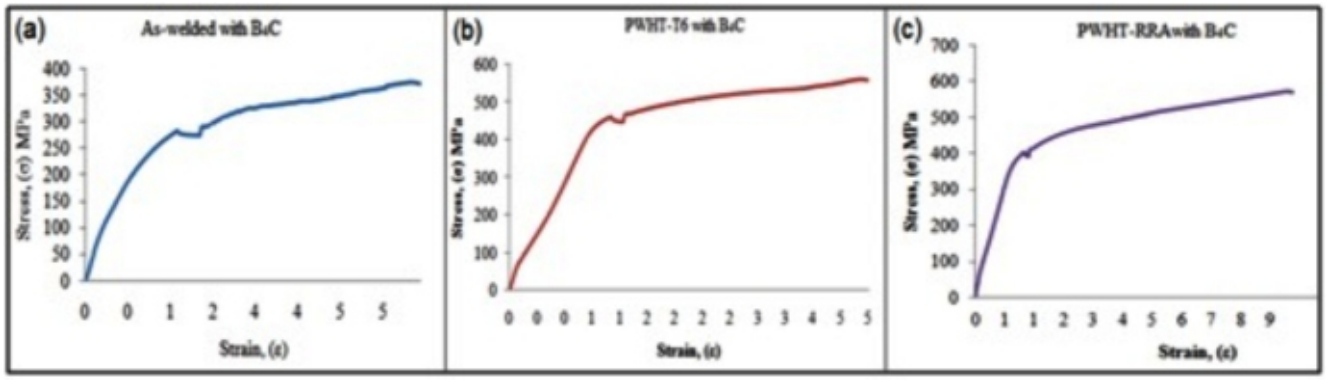

Fig.9 : Stress-strain curves of AA7075 aluminium alloy friction stir welds with B_4C nano powder addition : (a) As-welded, (b) PWHT-T6 and (c) PWHT-RRA

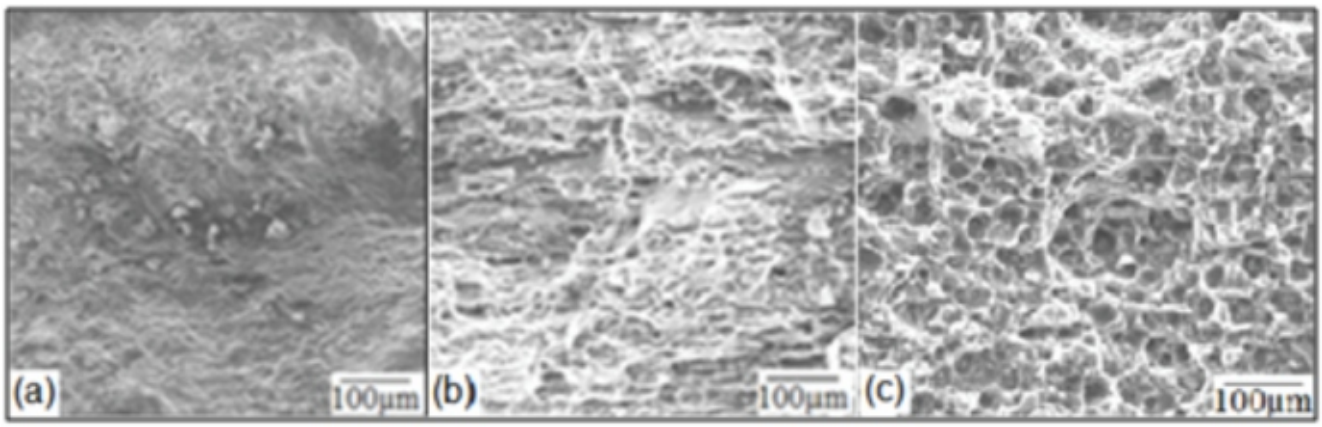

Fig.11 : SEM Fractographs of fractured SCC samples of welds without B_4C nano powder addition: (a) As-welded, (b) PWHT-T6 and (c) PWHT-RRA

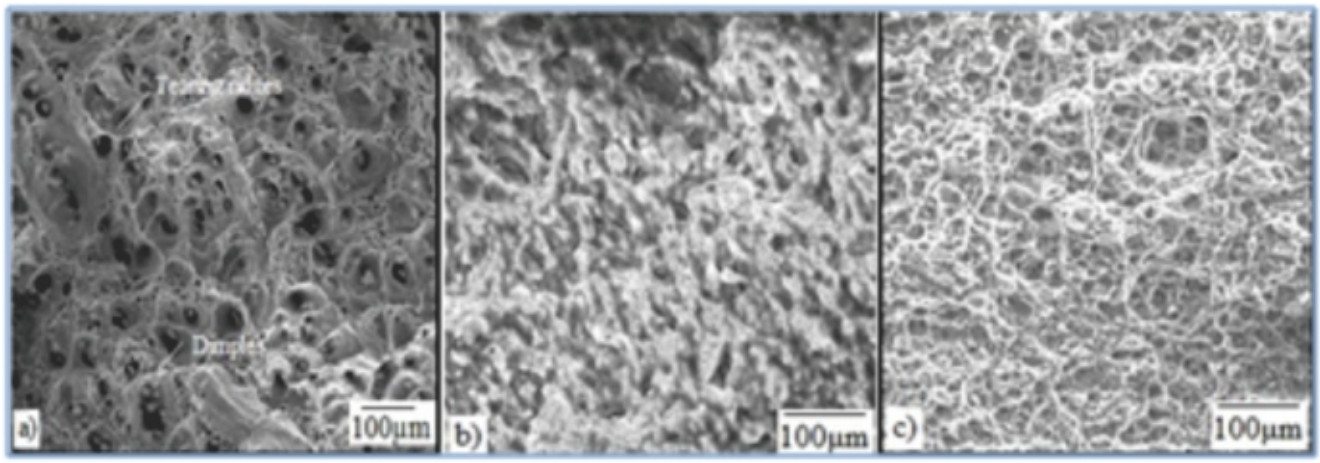

Fig. 12 : SEM Fractographs of fractured SCC samples of welds with B_4C nano powder addition: (a) As-welded, (b) PWHT-T6 and (c) PWHT-RRA

was failed in 5376 hours which is longer when compared to the PWHT-RRA sample without B_4C addition (4416 hours). The reinforcement of friction stir welds with finer B_4C particles followed by RRA treatment is found effective in reducing the susceptibility to both SCC and pit initiation without effecting the strength and hardness. RRA treatment reduces the SCC susceptibility by reduced pit initiation. B_4C reinforcement to the weld nugget further improved the mechanical properties. In addition, nano B_4C particles accumulate along the grain interiors. The nano particles act as barrier to the galvanic cell formation leading to the reduced conductivity between the matrix and the precipitates. Due to the combined effect of RRA and B_4C reinforcement, the mechanical properties and resistance to SCC were further improved when compared to the un-reinforced welds.

3.5 Fractography

SEM analysis was performed on the fractured SCC samples of aluminium 7075 alloy friction stir welds and is shown in the **Fig. 11** and **Fig. 12**. **Fig. 11(a)** shows Fractured welded SCC samples in various temper conditions. Fracture surface of the PWHT-T6 sample **(Fig. 11(b))** is dominated by the transgranular fracture with severe corrosion, showing the typical brittle fracture and SCC attack.

It is a typical brittle fracture, indicating that the toughness of 7075 alloy at PWHT-T6 state is poor. In the RRA sample the dimples nearly disappeared and the fracture surface is characterized by the intergranular micro void coalescences and cleavage facets. The predominance of the intergranular fracture suggests that the grain boundaries are the preferential

paths for the SCC **(Fig. 11 (b)**). From the **Fig. 12**, large population of dimples and tear ridges are observed in the fractograph of as-welded sample which suggests that the failure is ductile mode. PWHT-T6 fractured surface of the tensile specimens contains a large population of shallow and small dimples whereas fracture surface of as welded joints have small population of deep and elongated dimples. In the PWHT-RRA sample the fracture surface is characterized by the intergranular micro void coalescences and cleavage facets.

From the above results, boron carbide nano powders can be added to the weld nugget of A7075 aluminium alloy using FSW effectively. Presence of boron carbide powder in the WN significantly improved the hardness, tensile properties, pitting corrosion resistance and SCC resistance when compared to un-reinforced WN formed by FSW. The combined effect of post weld heat treatment of RRA and boron carbide addition significantly improved the stress corrosion cracking resistance without the loss of mechanical properties.

4.0 CONCLUSIONS

Friction stir welds of AA7075 aluminium alloy showed fine grain microstructure and the shape and morphology of aluminium grains were significantly affected by post weld heat treatments.

There is an improvement in the tensile strength in RRA sample close to the strength of T6 sample. RRA treatment with the addition of boron carbide powder resulted in improving the hardness of weld nugget and the increased hardness is attributed to the uniform distribution of strengthening precipitates in the matrix and particle strengthening.

After RRA, due to the discontinuous grain boundary precipitates with large spacing, no continuous chain exists for corrosion to take place. As a result, the susceptibility to pitting corrosion is reduced in the RRA samples.

SCC studies revealed that RRA post weld treatment significantly improved the SCC resistance. RRA treatment produced the weld strength equal to T6 strength and also higher resistance to the SCC than T6 sample.

Tensile strength and SCC resistance is improved in B_4C added welds after RRA treatment when compared to the same welds without B_4C addition. Addition of boron carbide nano particles in the weld nugget improved the SCC resistance after RRA treatment.

Optimum combination of strength and corrosion resistance of armour grade AA7075 Al-alloy friction stir weld can be achieved by the addition of B_4C powder and post weld heat treatment of RRA.

REFERENCES

[1] Sharma C, Dwivedi DK, Kumar P (2012); Effect of welding parameters on microstructure and mechanical properties of friction stir welded joints of AA7039 aluminum alloy, Mater Des, 36, pp.379-390.

[2] Paglia CS, Buchheit RG (2008); A look in the corrosion of aluminum alloy Friction stir welds, Scr Mater, 58, pp.383-387.

[3] Karaaslan A, Kaya I, Atapek H (2007); Effect of aging temperature and of retrogression treatment time on the microstructure and mechanical properties of alloy AA 7075, Metal Sci Heat Treat, 49, pp.9-10.

[4] Venugopal T, Srinivasa Rao K, Prasad Rao K (2004); Studies on friction stir welded AA7075 aluminum alloy. Trans Indian Inst Metals, 57 (6), pp.659-663.

[5] Rao K Srinivasa, Rao K Prasad. (2004); Pitting corrosion of heat-treatable aluminium alloys and welds: a review, Trans Indian Inst Met, 57 (6), pp.593-610.

[6] Ranganatha R (2013); Multi-stage heat treatment of aluminum alloy AA7049. Trans Nonferrous Met Soc China, pp.1570-1575.

[7] Su JQ, Nelson TW, Mishra R, Mahoney M (2003); Microstructural investigation of friction stir welded 7050- T651 aluminium, Acta Mater, 51(3), pp.713-729.

[8] Hassan KhAA, Norma AF, Price DA, Prangnell PB (2003); Stability of nugget zone grain structures in high strength Al-alloy friction stir welds during solution treatment. Acta Mater, 51 (7), pp.1923-1936.

[9] Sullivan A, Robson JD (2008); Microstructural properties of friction stir welded and post weld heated 7449 aluminum alloy thick plate. Mater Sci Eng (A), 478, pp.351-360.

[10] Oliveira Jr AF, de Barros MC, Cardoso KR, Travessa DN (2004); The effect of RRA on the strength and SCC resistance on AA7050 and AA7150 aluminum alloys, Mater Sci Eng, 379 (A), pp.321-326.

[11] Fuller CB, Mahoney MW, Calabrese M (2010); Evolution of microstructure and mechanical properties in naturally aged 7050 and 7075 Al friction stir welds, Mater Sci Eng, 527 (9), pp.2233-2240.

[12] Bahrami M, Dehgani K, Givi MKB (2014); A novel approach to develop aluminum matrix nano composite employing friction stir welding technique, Mater Des, 53, pp.217-225.

[13] Azimzadegan T, Khalaj GH, Kaykha MM. Heidari AR (2011); Ageing behavior of friction stir welding AA7075-T6 aluminum alloy, Comput Eng Syst Appl ,Vol. II, pp.183-187.

[14] Choi DH, Kim Y-Il, Kim DU (2012); Effect of SiC particles on microstructure and mechanical property of friction stir processed AA6061-T4, Trans Nonferrous Metal Soc China, 22(3), pp.614-618.

[15] Su JQ, Nelson TW, Sterling CJ (2005); Microstructure evolution during FSW/FSP of high strength aluminum alloys, Mater Sci Eng A, 405(1-2), pp.277-286.

[16] Gan YX, Solomon D, Reinbolt M (2010); Friction stir processing of particle reinforced composite materials, Materials, 3(1), pp.329-350.

[17] Ramesh R, Murugan N (2010); Microstructure and metallurgical properties of aluminium 7075 - T651 alloy/B_4C 4 % vol. surface composite by friction stir processing, Adv Mater Manuf Charact, 3(1), pp.301-306.

[18] Zaid HR, Hatab AM, Ibrahim AMA (2011); Properties enhancement of Al-Zn-Mg alloy by retrogression and re-aging heat treatment. J Min Metal, 47 (1), pp.31-35.

[19] Kashani-Bozorg SF, Jazayeri K (2008); Formation of Al/B_4C surface nano composite layers on 7075 Al alloy employing friction stir processing. AIP Conf Proc, 1136 (1), pp.715-719.

[20] Shafiei-Zarghani A. (2009); Microstructures and mechanical properties of Al/Al2O3 surface nano-composite layer produced by friction stir processing, Mater Sci Eng A, 500, pp.84-91.

ACKNOWLEDGEMENT

Authors would like to thank Director, Defence Metallurgical Research Laboratory for his encouragement and support to publish this work.